Korea-Australia Rheology Journal
Vol. 20, No. 3, September 2008 pp. 97-107

Structure, stability and applications of colloidal crystals

Masaki Yanagioka and Curtis W. Frank*
Department of Chemical Engineering, Stanford University, Stanford, California 94305-5025
(Received April 18, 2008)

Abstract

This article presents an overview of current research activities that center on colloidal crystals resulting from self-assembly of surface-charged nanoparticles. It is organized into three parts: the first part discusses characterization of colloidal structures, the second part describes colloidal stability from the rheological aspects of colloidal crystals suspended in medium, and the third part highlights polymerized colloidal crystals as a promising application. Finally, we briefly discuss the directions of future research in this area.

Keywords : colloidal crystals, stability of colloids, crystal structure, rheology

1. Introduction

Structure and physical properties of colloids have been studied intensively, since colloidal systems are important in various fields of industry and as models of solid and liquid structures for the study of phase transition behavior (Medeiros e Silva and Mokross, 1980; Hao, 2005). The most studied colloidal systems consist of monodisperse nanoparticles, which spontaneously self-assemble under appropriate conditions. Systems of these monodisperse particles exhibit interesting diffraction phenomena and are referred to as colloidal crystals. The colloidal crystals are roughly divided into close-packed and non-close-packed categories. The close-packed crystals comprise particles that are in contact with each other, and one of the approaches to form a close-packed crystal is to utilize evaporation-induced self-assembly driven by capillary forces (Gu *et al.*, 2002; Nakamura *et al.*, 2006). The shimmering wings of butterflies and iridescent opals are examples of the close-packed crystals found in nature.

Non-close-packed crystals are achieved by enhancing the surface charge on the particles such that they electrostatically repel one another. Here, colloidal crystals are regarded as being soft due to the surrounding electrical double layer, which plays an important role in the ordering process. Aqueous suspensions of colloidal polystyrene or silica particles are good examples of such suspensions. Typically, these particles are negatively charged, with counterions from the medium adsorbed onto the particles to neutralize the surface charge. By removing the counterions in the bulk solution using dialysis and ion-exchange resin (Goodwin *et al.*, 1980), the surface charge on the particle becomes unscreened and is enhanced, resulting in electrostatic repulsion among the particles. Because the volume of the colloidal dispersion is limited, the particles take the lowest possible energy configuration, which is a highly ordered crystal structure. Since this electrostatic repulsion exerts a long-range force upon the particles, the average interparticle distance can be as long as the order of the wavelength of light, depending on the volume fraction and the electrolyte concentration in the medium. Therefore, these colloidal crystals exhibit iridescence arising from the Bragg diffraction of visible light, and light scattering can be used to characterize the structural ordering. Compared to the close-packed crystals, the non-close-packed colloids are formed at much smaller volume fraction (Pusey and van Megen, 1986).

In this review, we first discuss characterization of colloidal structures because they form a basis for all properties of colloidal crystals. Next we describe the stability of the colloidal crystals from the viewpoint of their rheological properties. Then we will highlight polymerized colloidal arrays, where colloidal crystals are embedded in a polymeric matrix. Finally, we conclude with some comments on the directions towards which future research in this area might be focused.

2. Discussions

2.1. Colloidal structure

Any detailed understanding of interparticle interactions in colloidal suspensions will require the determination of the crystal structure. Depending on the volume fraction and the salt concentration, the suspension can undergo order-disorder transitions from a fluid state to a highly organized crystal of either body-centered cubic (BCC) or face-centered cubic (FCC) structure. Since the characterization

*Corresponding author: curt.frank@stanford.edu

of colloidal structures was first discussed in detail using Bragg diffraction by Hiltner and Krieger (1969), intensive research has been conducted on colloidal crystals. Determination of the colloidal structure has been achieved by Bragg diffraction (Reese *et al.*, 2001), Kossel diffraction (Kremer *et al.*, 1986; Robbins *et al.*, 1988; Rundquist *et al.*, 1989; Monovoukas and Gast, 1989), light scattering (Heimer and Tezak, 2002), or x-ray scattering (Matsuoka *et al.*, 1991; Konishi and Ise, 2006; Men *et al.*, 2006; Reichelt *et al.*, 2008), and some of the representative studies are reviewed in this paper.

2.1.1. Kossel diffraction

Generally, irradiation of the ordered colloidal crystal dispersion with visible light leads to Bragg diffraction. In addition to Bragg diffraction, Carlson and Asher (1984) took advantage of the so-called Kossel rings in order to determine the colloidal structure. The laser light scatters isotropically within the sample, but some portion of the scattered light that satisfies the Bragg angle cannot propagate through the sample. The dark Kossel rings, thus, result from this inability of the scattered light to propagate along directions that satisfy the Bragg condition. In addition to the dark Kossel rings, multiple Bragg diffraction leads to formation of the broadened bright Kossel rings, which are located outside the dark Kossel rings. The mechanism of the Kossel ring formation is shown in Fig. 1.

Colloidal crystal dispersion of polystyrene spheres was formed by removing excess ions from an aqueous

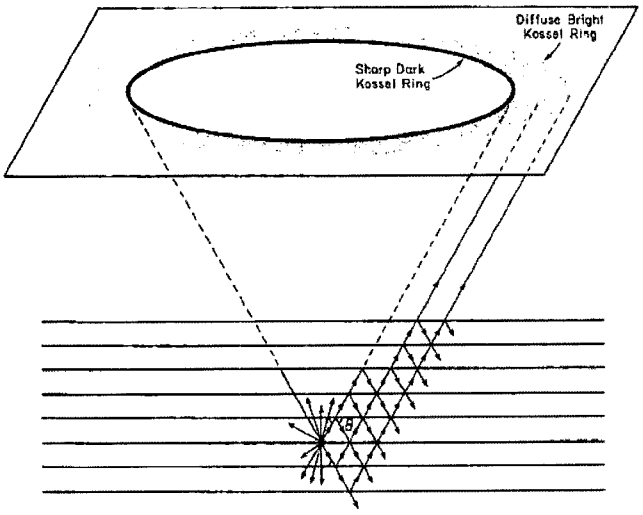

Fig. 1. Formation of bright and dark Kossel rings. Isotropic scattering of the laser light results in a divergent light source within the sample. The light at the Bragg angle θ is diffracted and cannot propagate through the lattice. Thus, dark Kossel rings are projected onto a target screen. The bright Kossel rings are considerably broadened by multiple Bragg diffraction. Reprinted with permission from (Carlson and Asher, 1984). Copyright © 1984 Society for Applied Spectroscopy.

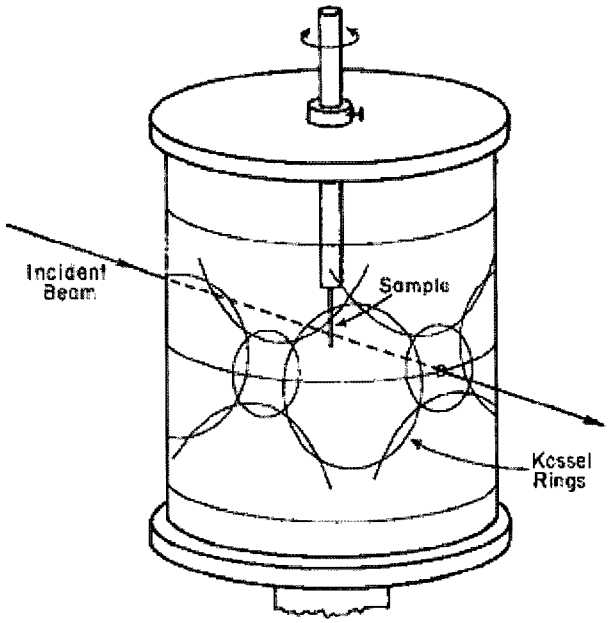

Fig. 2. Experimental apparatus showing Kossel ring patterns. Reprinted with permission from (Carlson and Asher, 1984). Copyright © 1984 Society for Applied Spectroscopy.

suspension of polystyrene spheres using dialysis and ion-exchange resin. Carlson and Asher (1984) placed a capillary that contained the colloidal crystal dispersion in a cylindrical sample container and irradiated the capillary with argon-ion laser (Fig. 2). On the wall of the container, they observed a series of Kossel rings that accompanied the Bragg diffraction spots. These Kossel rings are the trajectories of dark lines resulting from the intersection of surfaces of cones with the cylindrical screen around the sample chamber. The light is scattered within the sample; therefore, the apex of each cone also locates in the sample.

Investigation of these rings enabled Carlson and Asher to determine simultaneously both the crystal structure and orientation. They demonstrated that the interparticle distance in the crystals was many times larger than the sphere diameter and that the electrostatic repulsion was indeed the driving force of the formation of the non-close-packed colloidal crystals.

2.1.2. Fluorescence confocal scanning laser microscope (CSLM)

In the 1990's, a new type of light microscope, a fluorescence confocal scanning laser microscope (CSLM), was introduced into colloid science to study concentrated colloidal crystals. Verheagh *et al.* (1995) characterized colloidal systems of sterically stabilized silica spheres that crystallized into close-packed structures. Structure analysis by conventional light microscopy is not useful for these concentrated colloidal crystals, since the intensity of light is strongly reduced by scattering. The CSLM rejects light that does not come from the focal plane, and this permits

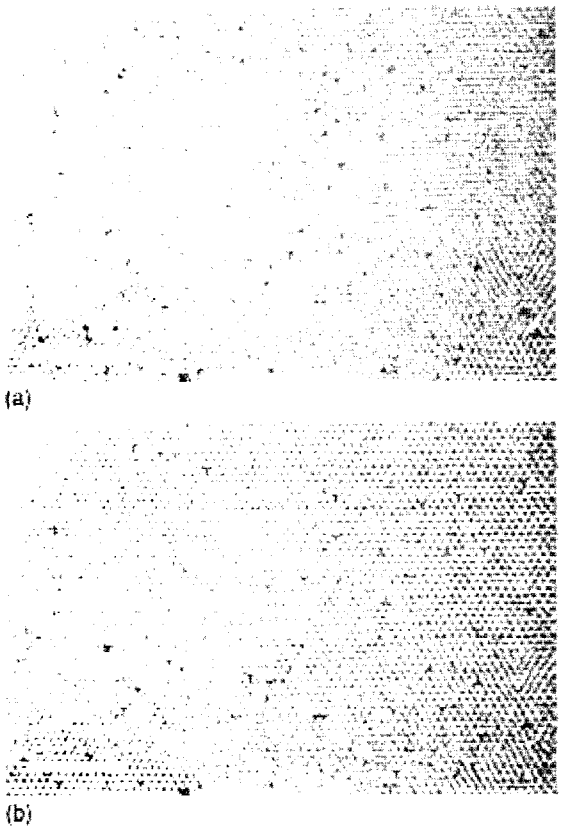

Fig. 3. Confocal scanning laser micrographs of a polycrystalline optical section in a 7 vol% dispersion of rhodamine-labeled silica spheres in chloroform. (a) Micrograph taken at a depth of about 20 μm below the glass wall. (b) Micrograph taken 0.4 μm below the previous one. Scale bar = 10 μm. Reprinted with permission from (Verhaegh *et al.*, 1995). Copyright © 1995 American Institute of Physics.

optical slicing and construction of three-dimensional images. This feature provides direct three-dimensional structural information in the mesoscopic range. Fig. 3 shows CLSM images of silica colloidal crystals taken at different depths below the cover glass.

Recently, Mohanty *et al.* (2005) have investigated the gas-liquid transition in highly charged colloidal polystyrene particles suspended in water by utilizing CLSM. They took images of the disordered suspension by CLSM, and demonstrated that it has voids in the dense disordered (amorphous) regions (Fig. 4). This is a direct observation of the inhomogeneous state, and it provides helpful information on the gas-liquid transition.

2.1.3. Static light scattering

Light-scattering can be used to investigate the ordering and the structure in colloidal dispersions because the interparticle distance of colloidal crystals is of the order of the wavelength of light (Heimer and Tezak, 2002). We will next briefly review how the scattering intensity $I_s(Q)$ is analyzed to obtain the static structure factor $S(Q)$, where light scatters from a scattering volume V_s containing N

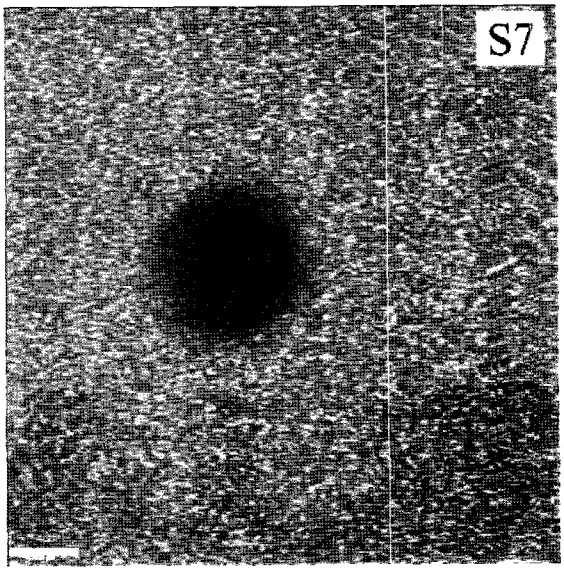

Fig. 4. CLSM image after averaging over 20 frames shows coexistence of voids (dark region) with dense disordered regions (gray region) for the highly charged polystyrene particles taken at a distance of 60 μm from the cover glass. Images are taken using λ=488 nm of Ar-ion laser and a 40× /0.75 objective. Scale bar=20 μm. Reprinted with permission from (Mohanty *et al.*, 2005). Copyright © 2005 American Chemical Society.

spherical colloidal particles. The static structure factor $S(Q)$ enables us to identify the colloidal structure.

Compared to the light scattered by the colloidal particles, the light scattered by the solvent is negligibly smaller. The following Rayleigh-Gans approximation for the time-averaged intensity is commonly used under this condition (Arora Akhilesh and Tata, 1998):

$$I_s(Q) = A_s P(Q) S(Q), \tag{1}$$

$$Q = \frac{4\pi\mu_m \sin(\theta/2)}{\lambda}, \tag{2}$$

where Q is the scattering wave vector, μ_m is the refractive index of the medium, and λ is the incident wavelength. In equation (1), $P(Q)$ is the particle-scattering form factor, $S(Q)$ is the interparticle structure factor, and A_s is a constant determined by various factors, such as the refractive indices of the particle and the medium, the particle concentration, the volume of the particle, the intensity of the incident radiation, and the distance between the scattering volume and the detector. The form factor $P(Q)$ for a spherical particle of radius a is given as

$$P(Q) = \left[\frac{3[\sin(Qa) - Qa\cos(Qa)]}{(Qa)^3}\right]^2. \tag{3}$$

The static structure factor $S(Q)$ is given by

$$S(Q) = 1 + \frac{1}{N}\sum_{i>j=1}^{N} \exp[iQ\cdot(r_i - r_j)], \tag{4}$$

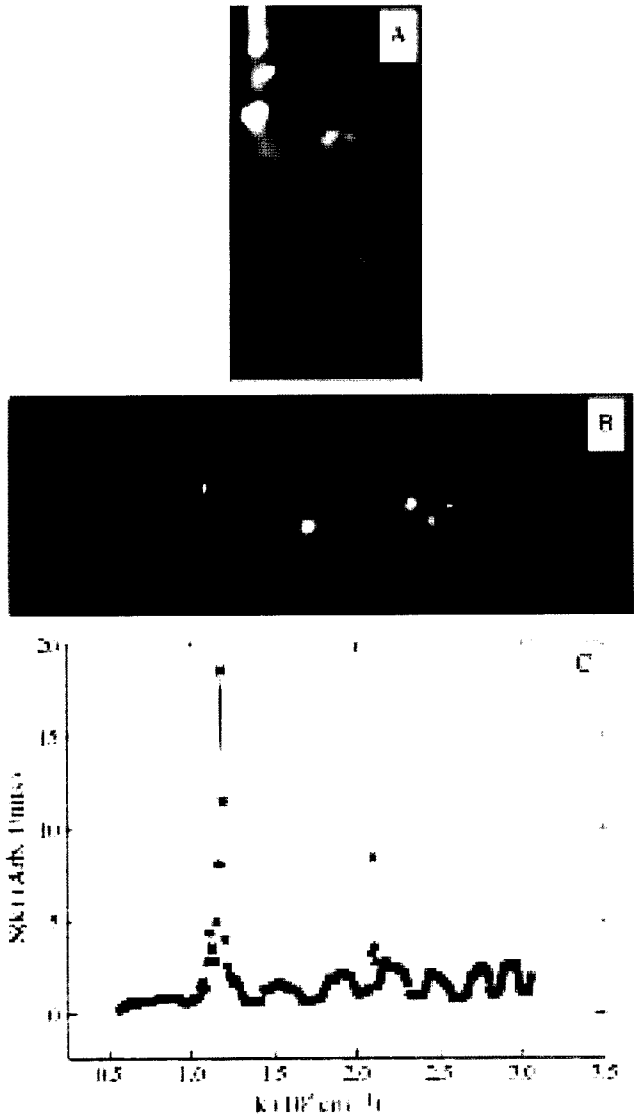

Fig. 5. (a) Iridescence from a charged colloidal crystal of polystyrene spheres (d=112 nm) dispersed in deionized water. (b) Bragg spots captured on a screen from colloidal crystals when illuminated with 514.5 nm argon-ion laser line. (c) Structure factor $S(k)$ vs. scattering wave vector k obtained from static light scattering shows sharp peaks corresponding to a BCC ordering in a colloidal crystal. Reprinted with permission from (Tata and Jena, 2006). Copyright © 2006 Elsevier Limited.

where r_i is the position of the center of mass of the i-th particle.

The static structure factor $S(Q)$ is obtained by measuring $I_s(Q)$ and then correcting for the form factor $P(Q)$ and the constant A_s using equation (1). Utilizing the static light scattering technique, Tata and Jena (2006) obtained the static structure factor $S(Q)$ for a charged colloidal crystal of polystyrene spheres dispersed in water. As shown in Fig. 5, their colloidal crystals exhibit iridescence resulting from the Bragg diffraction of visible light. In Fig. 5(c), they observed sharp peaks in the $S(Q)$, corresponding to a BCC structure.

2.1.4. Ultra-small-angle x-ray scattering (USAX)

The study of Tata and Jena (2006) clearly demonstrates that static light scattering is a powerful technique for identifying the colloidal structure, but, unfortunately, it is almost powerless when the samples are turbid and at relatively high concentrations. In this case, small-angle x-ray scattering (SAXS) (Reichelt *et al.*, 2008) and small-angle neutron scattering (SANS) (Ackerson *et al.*, 1986) have been used to determine the colloidal structure. However, the maximum dimension that may be measured by these two techniques is below sub-micron size because of the short wavelength of x-ray beams and of the low small-angle resolution of the apparatus. To counteract this, an ultra-small-angle x-ray scattering (USAX) technique has been developed for the measurement of micrometer-size domains (Matsuoka *et al.*, 1991; Konishi and Ise, 2006; Men *et al.*, 2006). This technique is based on the x-ray camera that was first reported by Bonse and Hart (1965). This geometry permits probing a wide angular range (3-4 orders of size) and, therefore, sizes up to 1 μm can be measured.

Men and co-workers (Men *et al.*, 2006) used a dispersion of soft spheres (styrene/butadiene copolymer) with a diameter of 135 nm to synthesize a crystalline film. The colloidal structure of this film was determined to be FCC by utilizing USAX, which they also used *in-situ*, while stretching the film in order to investigate the structural evolution of the colloid during macroscopic deformation. Because this technique is capable of probing dimensions of the order of micrometers, they were able to detect the structural evolution of the colloidal crystals under extension (Fig. 6). Based upon their observation, there is a deviation between the macroscopic and the crystal-

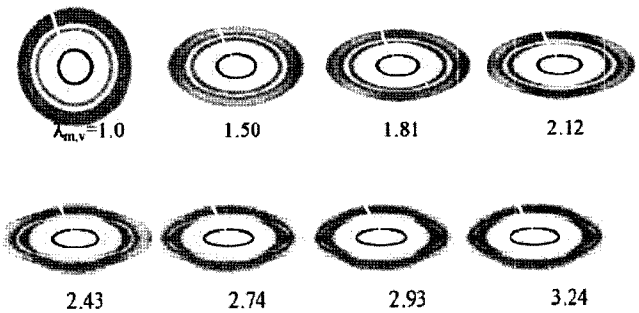

Fig. 6. Selected USAXS patterns taken during stretching of the latex film indicating the structural evolution of the colloidal crystallites under extension. The macroscopic elongation ratio ($\lambda_{m,v}$) is indicated on each pattern. (The tensile direction is vertical.) Reprinted with permission from (Men *et al.*, 2006). Copyright © 2006 American Chemical Society.

lographic draw ratios, which suggests non-affine deformation. They attributed this non-affine deformation to slippage between rows of particles and grain boundaries. This is a good example of the promising capability of USAX, especially when we deal with the colloidal crystal at relatively high concentrations.

2.2. Colloidal stability

As described in the introduction, the driving force for formation of colloidal crystals is electrostatic repulsion among particles, with the ordering influenced by many parameters, such as particle volume fraction (Carlson and Asher, 1984), surface charge density (Goodwin *et al.*, 1980), polydispersities of size and charge, ionic impurities (Hiltner and Krieger, 1969), shear (Ackerson and Clark, 1981; Butler and Harrowel, 1995), electric (Medebach and Palberg, 2003) and magnetic fields (Hayter *et al.*, 1989). Under certain conditions, therefore, one needs to determine how much the colloidal crystals are stable against these perturbations. Methods to investigate the colloidal stability can be roughly divided into direct monitoring of particle size and an indirect approach using rheological properties of particle suspensions.

Particle size can be directly monitored by light scattering as long as there is sufficient difference in the refractive indices between colloidal particles and the suspending media. Heimer and Tezak (2002) evaluated the dynamics of aggregation of colloidal silver iodide particles by the static light scattering method. This approach enabled the use of Zimm plots in order to determine the radii of spherical particles. Stable silver iodide colloids showed the usual Zimm diagrams, while the diagrams were distorted when the stability of the colloids decreased. The colloid stability of polydispersed aggregates was explained using the second virial coefficient, its negative sign implying interaction of particles in the solution, its positive value indicating formation of new particles from the supernatant solution.

Compared to the light scattering method, the rheological method is rather indirect, yet it has provided accurate information on the stability of colloidal suspensions. In particular, the shear-thinning behavior of colloidal suspensions, or the viscosity decrease with increasing shear rate, has been investigated for more than 50 years. This non-Newtonian behavior has been attributed to mechanisms in which the shear stress orients or distorts the suspended particles in opposition to the randomizing effects of Brownian motion (Craciun *et al.*, 2003). In other words, this phenomenon involves a competition between shearing and thermal forces, and the size of the suspended particle plays a determining role in this competition.

Krieger *et al.* (Krieger and Dougherty, 1959; Krieger and O'Neill, 1968) investigated the cause of this non-Newtonian behavior of colloidal particles and developed a theory that focused on the interactions between two neighboring particles. The key essence of their argument lies in quantitative treatment of the formation and dissociation of "doublets", a pair of spheres that tends to rotate as a dumbbell in the medium. If the separation between two spheres permits them to rotate independently of each other, the spheres will be called "singlets" (Fig. 8).

In the absence of shearing forces, the distribution of singlets and doublets can be represented as a chemical equilibrium:

$$2P_1 \underset{k_d}{\overset{k_f}{\rightleftarrows}} P_2, \tag{5}$$

where P_1 is a singlet, P_2 is a doublet, and k_f and k_d represent the specific rate constants for the formation and dissoci-

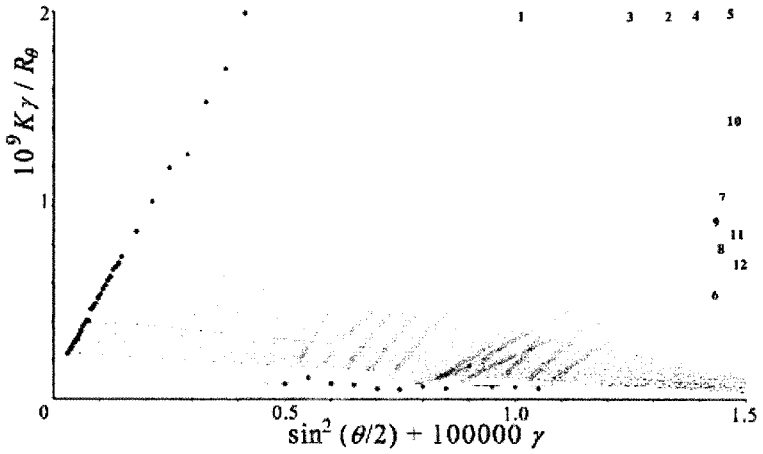

Fig. 7. Zimm plot of the positively charged silver iodide colloids 10 min after preparation of samples. Open circles represent the experimental data; the extrapolated values are represented by filled circles. Units relating to the axes: *x*-axis: concentrations (g) are expressed in g cm^{-3}; *y*-axis: mol g^{-1}. Reprinted with permission from (Heimer and Tezak, 2002). Copyright © 2002 Elsevier Limited.

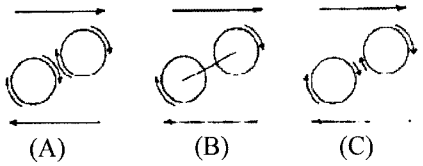

Fig. 8. (A) Schematic diagram of flow pattern if nearby spheres were to rotate independently. (B) Schematic flow pattern if they were to rotate as rigid dumbbell. (C) Diagram of actual flow pattern. Reprinted with permission from (Krieger and Dougherty, 1959). Copyright © 1959 The Society of Rheology.

ation of doublets, respectively.

In the presence of shearing forces, however, a second mechanism for the decomposition of doublets is introduced, since they will be separated during the dumbbell rotation.

$$P_2 \xrightarrow{k_s} 2P_1, \tag{6}$$

where k_s is the specific rate constant for the shear-induced dissociation.

They developed a careful argument by focusing on the competition between the shearing and thermal forces acting on a pair of particles, and their resultant flow equation (not shown here) successfully predicted the shear-thinning behavior of butadiene/styrene latex suspensions at various volume fractions, v, of colloidal particles (Fig. 9). They concluded that "crowding" of particles plays a vital role in the origin of this shear-thinning behavior. Their word "crowding" should represent the formation of

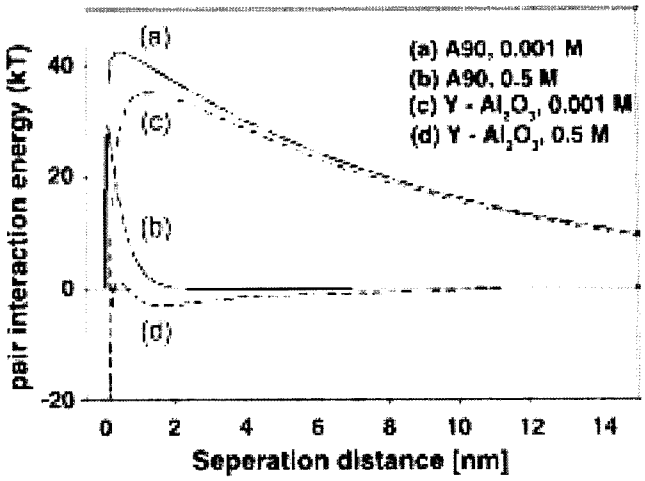

Fig. 10. Calculated DLVO pair interaction energy curves for silica and γ-alumina, based on a spherical geometry with a particle diameter of 20 nm and a Stern potential of 85 mV. Reprinted with permission from (Paik *et al.*, 2005). Copyright © 2005 Elsevier Limited.

colloidal structure, and their "singlet-doublet" approach emphasizes the significance of the interparticle interactions in the rheological behavior.

Krieger's approach (Krieger and Dougherty, 1959) concentrates on the competition of shearing and thermal forces, but another approach is also possible by specifically dealing with the colloidal forces that arise from enhanced electrostatic repulsion among charged particles. According to Derjaguin–Landau–Verwey–Overbeek (DLVO) theory (Stokes and Evans, 1997), colloidal forces are predicted

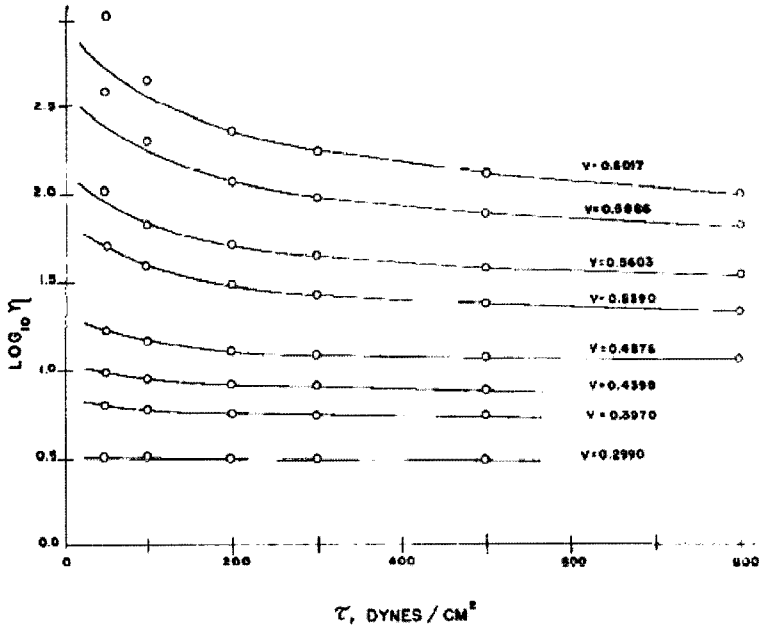

Fig. 9. Graphical comparison of observed (points) and calculated (solid line) viscosities using the experimental data of Maron and Shiu Ming (1955). Reprinted with permission from (Krieger and Dougherty, 1959). Copyright © 1959 The Society of Rheology.

well by combining two opposing forces between colloidal particles suspended in medium: (1) electrostatic repulsive forces, which result from unscreened surface charge on the particle, and (2) van der Waals attractive forces, which are universal in nature.

Paik *et al.* (2005) investigated the influence of the electrical double layer on the stability of the silica and γ-alumina suspension using DLVO theory. In order to alter the thickness of the electrical double layer, they prepared two levels of electrolyte concentrations (0.001M and 0.5M) for both suspensions. Fig. 10 shows the DLVO interaction energy calculated as a function of separation distance for silica and γ-alumina at two electrolyte concentrations. Here, silica suspensions are denoted by (a) and (b), and those for γ-alumina are (c) and (d). At low electrolyte concentration, both systems, (a) and (c), showed large repulsive energy barriers extending out more than 30 nm from the particle surface, and this represents high colloidal stability. At higher electrolyte concentration, however, the DLVO interaction energy decreased significantly for γ-alumina, (d), indicating an unstable system. In contrast, the corresponding curve for silica, (b), still exhibits a large repulsive barrier, which is sufficient to prevent extensive aggregation from occurring in this system.

In order to evaluate the accuracy of this DLVO prediction experimentally, Paik *et al.* measured the viscosity of γ-alumina and silica suspensions as a function of electrolyte concentration and shear rate (Figs. 11 and 12 respectively). For γ-alumina, the change in viscosity and shear thinning behavior with increasing ionic strength followed the expected DLVO prediction. In other words, with increasing ionic strength, viscosity continually rises and shear thinning becomes more enhanced. This is typical of unstable colloidal suspensions.

Silica, on the other hand, showed the opposite behavior to γ-alumina, where viscosity decreased and shear thinning behavior became smaller with increasing ionic strength. One might think that silica does not obey the DLVO prediction, but consideration of the particle "crowding" argument developed by Krieger and Dougherty (1959) demystifies this phenomenon. As we can see in the DLVO interaction energy (Fig. 10), the silica colloidal crystal is very stable due to its low Hamaker constant by nature. Therefore, silica aggregation itself does not have much impact on viscosity; rather, the formation of an ordered structure, or "crowding" of silica particles, increased the viscosity at low shear rate. With increasing shear rate, the shear stress breaks the structure of the silica particles, resulting in shear-thinning behavior. At high shear rates, a limiting linear relation between shear stress and shear rate was observed, indicating that additional changes in structure do not occur beyond a critical shear. Addition of electrolyte causes the double layer to collapse, resulting in loss of structure, and a corresponding loss of viscosity and shear thinning behavior.

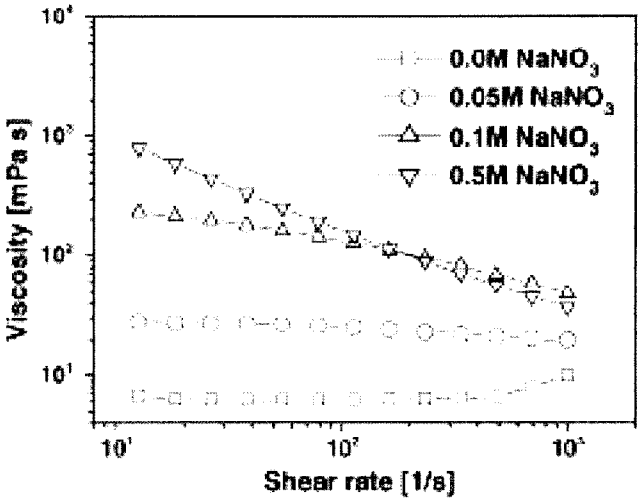

Fig. 11. The effect of electrolyte concentration on the viscosity of 13.2% γ-alumina at pH 5 as a function of shear rate. Reprinted with permission from (Paik *et al.*, 2005). Copyright © 2005 Elsevier Limited.

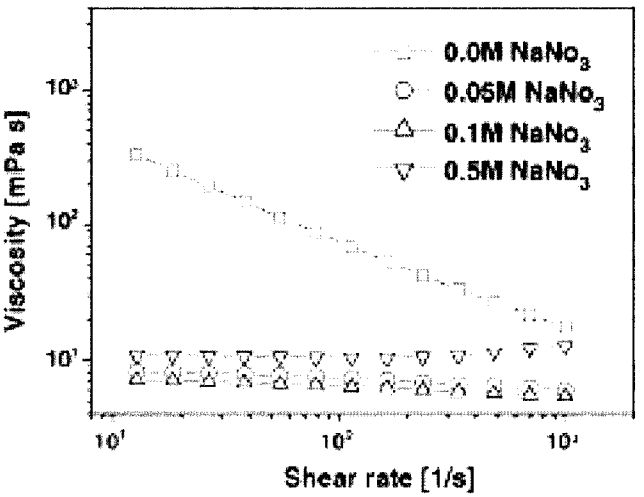

Fig. 12. The effect of electrolyte concentration on the viscosity of 13.2% A90 silica at pH 8 as a function of shear rate. Reprinted with permission from (Paik *et al.*, 2005). Copyright © 2005 Elsevier Limited.

2.3. Applications of colloidal crystals

Well-ordered crystalline arrays Bragg-diffract light efficiently. However, they will transiently disorder under shock or upon introduction of ionic impurities that screen the interparticle repulsive interactions. Thus, their long-term stability depends upon the cleanliness of their environment and their containers. Asher and co-workers (Weissman *et al.*, 1996; Holtz *et al.*, 1998) have developed an approach to permanently lock in the colloidal crystalline array (CCA) in a solid matrix. Into the CCA they intro-

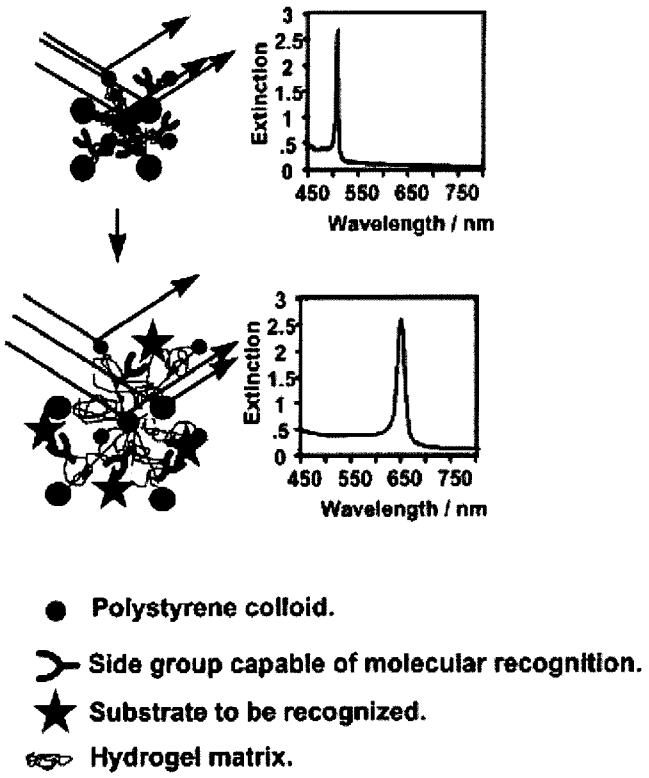

Fig. 13. General motif for the intelligent polymerized crystalline colloidal array (IPCCA) sensors. The CCA Bragg diffraction is a sensitive monitor of the hydrogel volume change induced by the interaction or binding of the molecular recognition agent to a substrate. In principle, any molecular recognition agent can be attached to the hydrogel polymer to produce an IPCCA sensor. Reprinted with permission from (Holtz *et al.*, 1998). Copyright © 1998 American Chemical Society.

duced purified nonionic monomers and initiators that can form a hydrogel network around the CCA spheres. This polymerized CCA (PCCA) forms a solid hydrogel that locks in the CCA periodic order; therefore, it remains stable in the presence of these polymerizable species provided that the monomers do not contain ionic impurities. The CCA polymerization results in only modest changes in the CCA ordering, as evidenced by the modest alterations of the diffraction peak. The hydrogel film is very stable. Addition of solutes does not perturb the array ordering since the lattice order no longer depends upon electrostatic interactions among spheres.

Asher and co-workers demonstrated that PCCA films exhibit significant changes in their optical characteristics with water content, which could be applied to optical filtering and sensors. The intelligent hydrogel incorporates chemical molecular recognition agents that cause the gel to swell in response to the concentration of particular analytes; the gel volume is a function of the analyte concentration. The color diffracted from the hydrogel film is, thus, a function of analyte concentration: the swelling of the gel changes the periodicity of the CCA, which results in a shift in the diffracted wavelength (Fig. 13).

Mechanically robust composite films composed of silica particles in acrylate polymers have been proposed by Foulger and co-workers (Foulger *et al.*, 2001) which exhibited a mechano-chromic response. During the mechanical testing of the PCCA films, the observation was made that the films exhibited color changes with deformation. They attributed this response to the compression of the lattice, where the nearest neighbor distance for the particles in the PCCA was calculated to be 2.6 times greater than the distance based on intimate contact of the particles. To explore this phenomenon more thoroughly, the film was then placed over an optical probe in which the reflectance spectra of the films could be observed at normal incidence.

Fig. 14 presents the reflectance spectra of a water-swollen PCCA film in the stress-free state and under compressive loading. In the initial stress-free state, the swelling of the films resulted in a diffraction peak movement from 542 to 580 nm. Upon application of a ca. 1 kPa compressive load, the diffraction peak shifts down to 525 nm, a 55 nm reduction. The removal of the load allows the film to immediately regain the optical characteristics of the original stress-free state. This material has a possible application as a sensitive pressure sensor.

A totally different approach of utilizing polymerized colloidal crystals can be taken by regarding them as a

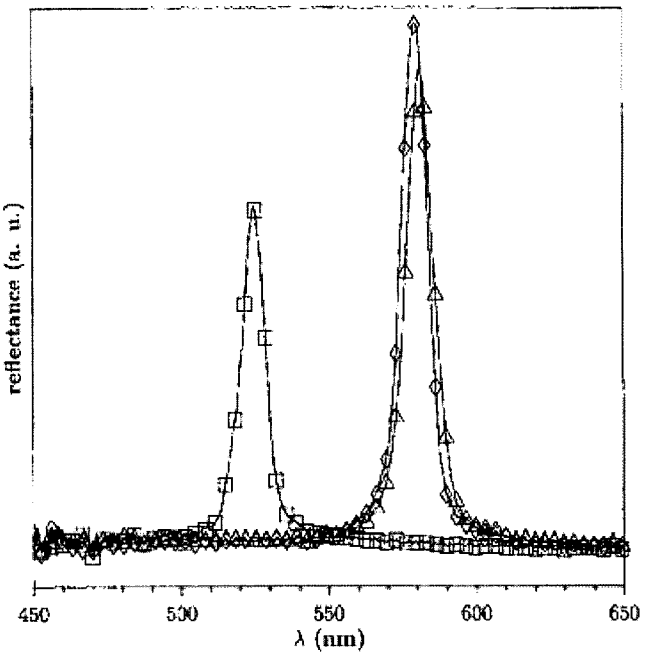

Fig. 14. Reflectance spectra of PCCA composite with compressive loading: original stress-free state (◇), under a ca. 1 kPa load (□), and unloaded stress-free state (△). Reprinted with permission from (Foulger *et al.*, 2001). Copyright © 2001 American Chemical Society.

model composite with perfect particle distribution. Incorporation of nanoparticles into polymeric materials reinforces the mechanical properties of the composite. Particle agglomeration has a big impact on their mechanical properties, but the quantitative relationship between the particle agglomeration and the mechanical properties of the composite is still unclear. The major reason for this ambiguous relationship lies in the coupling of the particle-matrix interaction and the particle distribution within the matrix. An attempt to change the particle agglomeration is usually achieved by altering the surface reactivity of nanoparticles; therefore, it is unclear whether the difference in the mechanical property upon the surface treatment of the particle arises from the resultant change of agglomeration or simply from the change of reaction between particles and the matrix. To counteract this, we prepared colloidal crystals in such a way as to obtain different particle distributions without changing the particle-matrix interactions (Yanagioka and Frank, 2008). The interparticle distance depends only upon the electrostatic repulsion. Therefore, variable particle dispersion may be achieved just by changing this repulsive force. This enables us to change the particle distribution without any effect upon the matrix-particle interaction.

We chose poly(*N*-isopropylarylamide) hydrogel as a matrix polymer, and incorporated silica particles (diameter of 110 nm) with two distinct distributions: the ordered distribution was made by utilizing the colloidal crystal of the silica and the random distribution was prepared by simply using the silica aqueous suspension. These two composites

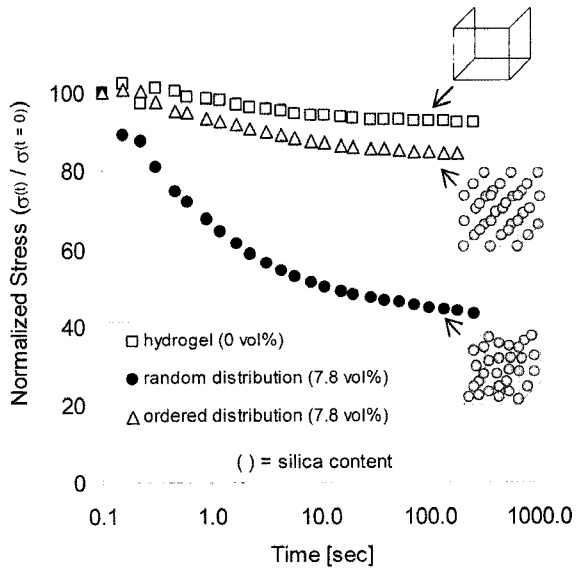

Fig. 15. (a) Stress relaxation curves at constant shear strain of 10% normalized by initial stress, $\sigma_{(t=0)}$, for the pure hydrogel, the hydrogel that has a random particle distribution, and the hydrogel that has an ordered particle distribution. Silica concentrations in the composites are indicated in parentheses in the inset.

had the same silica particles at the same volume fraction, and only the distribution was different. For comparison, we also synthesized the pure hydrogel.

In Fig. 15, stress relaxation curves are shown for the three materials, where constant shear strain of 10% was applied to the materials. Obviously, the stress relaxation is larger for the composite with random distribution than the one with ordered distribution. This must be caused by purely the difference of the particle distribution within the matrix, and it suggests that the de-agglomeration process of the random-silica composite is more prominent than the ordered-silica composite during the relaxation process. This study reveals significant effect of the particle distribution on the overall mechanical properties of the composite and further detailed investigation of other mechanical properties is now under way.

Ordered colloidal systems have lattice spacings ranging from nanometers to micrometers and can therefore diffract ultraviolet, visible, and near-infrared light. This appearance of long-range order of either BCC or FCC colloidal structure even at dilute concentration is the most fascinating phenomenon for the colloidal crystals. Therefore, one of the future directions of the research in this field should be related to this dramatic optical property. One example that takes advantage of the diffraction property is narrow-bandwidth filters composed of monodisperse polystyrene latexes in water, which can be used to reject the Rayleigh scattering in a Raman spectrometer (Flaugh *et al.*, 1984). There is a variety of other applications, including sensors (Holtz and Asher, 1997; Sharma *et al.*, 2004), optical limiters (Sunkara *et al.*, 1994), optical switches (Pan *et al.*, 1997), electrical switches (Gong and Marr, 2001), waveguides (Weissman *et al.*, 1996; Joannopoulos *et al.*, 1997; Chow *et al.*, 2000), photonic crystals (Norris and Vlasov, 2001; Iwayama *et al.*, 2003).

Other possible approaches that are not directly associated with their optical properties but are rather related to the structuring ordering include utilizing the collolidal crystals as templates for synthesis of novel materials (Velev *et al.*, 1997; Wijnhoven and Vos, 1998), and as model nanocomposites where we have essentially a perfect particle distribution, as described above. In particular, methods of using colloidal crystals as templates for preparing porous materials yield products with highly uniform and structured pores of tunable size in the submicron region. Such microstructured porous materials have potential applications in catalysis, filtering, coating, microelectronics, and electro-optics.

3. Summary

From what has been reviewed in this article, it is quite obvious that the field of colloidal crystals has attracted many researchers from viewpoints of both fundamental

science and application-oriented engineering. Characterization of colloidal structures was originally done by utilizing diffraction of visible light, but complementary techniques, such as CSLM and x-ray, or neutron scattering have also gathered considerable attention. CLSM reveals the internal structure of the colloidal crystals. In particular, USAX is a promising technique when we are interested in colloidal crystals, whose dimension falls onto a sub-micron range. The colloidal stability can be predicted reasonably well by the DLVO theory, and the detailed investigation of the stability may be conducted by the viscosity measurement. Finally, we discussed many possible applications of colloidal crystals from both optical and non-optical viewpoints. In order to understand the behavior of the colloidal structure and to achieve these novel applications, a deep knowledge about the particle-particle and the particle-polymer interactions is essential.

Acknowledgment

This work is supported by the Center on Polymer Interfaces and Macromolecular Assemblies (CPIMA), which is sponsored by an NSF-MRSEC program. M. Y. is grateful for support in the form of a fellowship from Bridgestone Corporation.

References

Ackerson, B. J. and N. A. Clark, 1981, Shear-induced melting, *Phys. Rev. Lett.* **46**, 123-126.

Ackerson, B. J., J. B. Hayter, N. A. Clark and L. Cotter, 1986, Neutron scattering from charge stabilized suspensions undergoing shear, *J. Chem. Phys.* **84**, 2344-2349.

Arora Akhilesh K. and B. V. R. Tata, 1998, Interactions, structural ordering and phase transitions in colloidal dispersions, *Adv. Colloid Interface Sci.* **78**, 49-97.

Bonse, U. and M. Hart, 1965, Tailless x-ray single-crystal reflection curves obtained by multiple relfection, *App. Phys. Lett.* **7**, 238-240.

Butler, S. and P. Harrowel, 1995, The shear induced disordering transition in a colloidal crystal: nonequilibrium Brownian dynamic simulations, *J. Chem. Phys.* **103**, 4653-4671.

Carlson, R. J. and S. A. Asher, 1984, Characterization of optical diffraction and crystal structure in monodisperse polystyrene colloids, *Appl. Spectrosc.* **38**, 297-304.

Chow, E., S. Y. Lin, S. G. Johnson, P. R. Villeneuve, J. D. Joannopoulos, J. R. Wendt, G. A. Vawter, W. Zubrzycki, H. Hou and A. Alleman, 2000, Three-dimensional control of light in a two-dimensional photonic crystal slab, *Nature* **407**, 983-986.

Craciun, L., P. J. Carreau, M. Heuzey, T. G. M. van de Ven and M. Moan, 2003, Rheological properties of concentrated latex suspensions of poly (styrene-butadiene), *Rheol. Acta* **42**, 410-420.

Flaugh, P. L., S. E. O'Donnell and S. A. Asher, 1984, Development of a new optical wavelength rejection filter: demonstration of its utility in Raman spectroscopy, *Appl. Spectrosc.* **38**, 847-850.

Foulger, S. H., P. Jiang, A. C. Lattam, D. W. Smith and J. Ballato, 2001, Mechanochromic response of poly(ethylene glycol) methacrylate hydrogel encapsulated crystalline colloidal arrays, *Langmuir* **17**, 6023-6026.

Gong, T. and D. W. M. Marr, 2001, Electrically switchable colloidal ordering in confined geometries, *Langmuir* **17**, 2301-2304.

Goodwin, J. W., R. H. Ottewill and A. Parentlich, 1980, Optical examination of structured colloidal dispersions, *J. Phys. Chem.* **84**, 1580-1586.

Gu, Z., A. Fujishima and O. Sato, 2002, Fabrication of high-quality opal films with controllable thickness, *Chem. Mater.* **14**, 760-765.

Hao, T., 2005, Electrorheological fluids: The non-aqueous suspensions, Elsevier, Amsterdam, p. 250.

Hayter, J. B., R. Pynn, S. Charles, A. T. Skjeltorp, J. Trewhella, G. Stubbs and P. Timmins, 1989, Ordered macromolecular structures in ferrofluid mixtures, *Phys. Rev. Lett.* **62**, 1667-1670.

Heimer, S. and D. Tezak, 2002, Structure of polydispersed colloids characterised by light scattering and electron microscopy, *Adv. Colloid Interface Sci.* **98**, 1-23.

Hiltner, P. A. and I. M. Krieger, 1969, Diffraction of light by ordered suspensions, *J. Phys. Chem.* **73**, 2386-2389.

Holtz, J. H. and S. A. Asher, 1997, Polymerized colloidal crystal hydrogel films as intelligent chemical sensing materials, *Nature* **389**, 829-832.

Holtz, J. H., J. S. W. Holtz, C. H. Munro and S. A. Asher, 1998, Intelligent polymerized crystalline colloidal arrays: novel chemical sensor materials, *Anal. Chem.* **70**, 780-791.

Iwayama, Y., J. Yamanaka, Y. Takiguchi, M. Takasaka, K. Ito, T. Shinohara, T. Sawada and M. Yonese, 2003, Optically tunable gelled photonic crystal covering almost the entire visible light wavelength region, *Langmuir* **19**, 977-980.

Joannopoulos, J. D., P. R. Villeneuve and S. Fan, 1997, Photonic crystals: putting a new twist on light, *Nature* **386**, 143-149.

Konishi, T. and N. Ise, 2006, Rupture and regeneration of colloidal crystals as studied by two-dimensional ultra-small-angle x-ray scattering, *Langmuir* **22**, 9843-9845.

Kremer, K., M. O. Robbins and G. S. Grest, 1986, Phase diagram of Yukawa systems: model for charge-stabilized colloids, *Phys. Rev. Lett.* **57**, 2694-2697.

Krieger, I. M. and T. J. Dougherty, 1959, A mechanism for non-newtonian flow in suspensions of rigid spheres, *J.Rheol.* **3**, 137-152.

Krieger, I. M. and F. M. O'Neill, 1968, Diffraction of light by arrays of colloidal spheres, *J. Am. Chem. Soc.* **90**, 3114-3120.

Maron, S. H. and F. Shiu Ming, 1955, Rheology of synthetic latex : V. flow behavior of low-temperature GR-S latex, *J. Colloid Sci.* **10**, 482-493.

Matsuoka, H., K. Kakigami, N. Ise, Y. Kobayashi, Y. Machitani, T. Kikuchi and T. Kato, 1991, Ultra-small-angle x-ray-scattering study: preliminary experiments in colloidal suspensions, *Proc. Nat. Acad. Sci. U.S.A.* **88**, 6618-6619.

Medebach, M. and P. Palberg, 2003, Phenomenology of colloidal

crystal electrophoresis, *J. Chem. Phys.* **119**, 3360-3370.
Medeiros e Silva, J. and B. J. Mokross, 1980, On the solid-like phase transition in crystals of polystyrene spheres in aqueous suspensions, *Solid State Commun.* **33**, 493-494.
Men, Y., J. Rieger, S. V. Roth, R. Gehrke and X. Kong, 2006, Non-affine structural evolution of soft colloidal crystalline latex films under stretching as observed via synchrotron x-ray scattering, *Langmuir* **22**, 8285-8288.
Mohanty, P. S., B. V. R. Tata, A. Toyotama and T. Sawada, 2005, Gas-solid coexistence in highly charged colloidal suspensions, *Langmuir* **21**, 11678-11683.
Monovoukas, Y. and A. Gast, 1989, The experimental phase diagram of charged colloidal suspensions, *J. Colloid Interface Sci.* **128**, 533-548.
Nakamura, H., M. Ishii, A. Tsukigase, M. Harada and H. Nakano, 2006, Close-packed colloidal crystalline arrays composed of silica spheres coated with titania, *Langmuir* **22**, 1268-1272.
Norris, D. J. and Y. A. Vlasov, 2001, Chemical approaches to three-dimensional semiconductor photonic crystals, *Adv. Mater.* **13**, 371-376.
Paik, U., J. Y. Kim and V. A. Hackley, 2005, Rheological and electrokinetic behavior associated with concentrated nanosize silica hydrosols, *Mater. Chem. Phys.* **91**, 205-211.
Pan, G., R. Kesavamoorthy and S. A. Asher, 1997, Optically nonlinear Bragg diffracting nanosecond optical switches, *Phys. Rev. Lett.* **78**, 3860-3863.
Pusey, P. N. and W. van Megen, 1986, Phase behaviour of concentrated suspensions of nearly hard colloidal spheres, *Nature* **320**, 340-342.
Reese, C. E., M. E. Baltusavich, J. P. Keim and S. A. Asher, 2001, Development of an intelligent polymerized crystalline colloidal array colorimetric reagent, *Anal. Chem.* **73**, 5038-5042.
Reichelt, H., C. A. Faunce and H. H. Paradies, 2008, The phase diagram of charged colloidal lipid A-diphosphate dispersions, *J. Phys. Chem. B* **112**, 3290-3293.
Robbins, M. O., K. Kremer and G. S. Grest, 1988, Phase diagram and dynamics of Yukawa systems, *J. Chem. Phys.* **88**, 3286-3312.
Rundquist, P. A., P. Photinos, S. Jagannathan and S. A. Asher, 1989, Dynamical Bragg diffraction from crystalline colloidal arrays, *J. Chem. Phys.* **91**, 4932-4941.
Sharma, A. C., T. Jana, R. Kesavamoorthy, L. Shi, M. A. Virji, D. N. Finegold and S. A. Asher, 2004, A general photonic crystal sensing motif: creatinine in bodily fluids, *J. Am. Chem. Soc.* **126**, 2776-2977.
Stokes, R. J. and D. F. Evans, 1997, Fundamentals of interfacial engineering, Wiley, New York, p. 145.
Sunkara, H. B., J. M. Jethmalani and W. T. Ford, 1994, Composite of colloidal crystals of silica in poly(methyl methacrylate), *Chem. Mater.* **6**, 362-364.
Tata, B. V. R. and S. S. Jena, 2006, Ordering, dynamics and phase transitions in charged colloids, *Solid State Commun.* **139**, 562-580.
Velev, O. D., T. A. Jede, R. F. Lobo and A. M. Lenhoff, 1997, Porous silica via colloidal crystallization, *Nature* **389**, 447-448.
Verhaegh, N. A. M., J. S. van Duijneveldt, A. van Blaaderen and H. N. W. Lekkerkerker, 1995, Direct observation of stacking disorder in a colloidal crystal, *J. Chem. Phys.* **102**, 1416-1421.
Weissman, J. M., H. B. Sunkara, A. S. Tse and S. A. Asher, 1996, Thermally switchable periodicities and diffraction from mesoscopically ordered materials, *Science* **274**, 959-963.
Wijnhoven, J. E. G. and W. L. Vos, 1998, Preparation of photonic crystals made of air spheres in titania, *Science* **281**, 802-804.
Yanagioka, M. and C. W. Frank, 2008, Effect of particle distribution on morphological and mechanical properties of filled hydrogel composites, *Macromolecules* **41**, 5441-5450.